*International Journal of Internet, Broadcasting and Communication Vol.7 No.1 75-92 (2015)*
*http://dx.doi.org/10.7236/IJIBC.2015.7.1.75*

**IJIBC 15-1-15**

# Application of Bond Valence Method to Estimate the Valence Charge Distribution in the Metal-to-Oxygen Bonding Spheres in Perovskites

*Hoang Nam Nhat[1], Dinh Van Chau[1*], Dinh Van Thuong[1], and Nguyen Thi Hang[1]*

*Faculty of Engineering Physics and Nanotechnology, VNU-University of Engineering and Technology, Vietnam*
dinhchau@vnu.edu.vn

***Abstract***

This paper presents the application of the bond valence method to estimate the valence charge distribution in several perovskite systems: $La_{1-x}Pb_xMnO_3$ (x=0.1-0.5), $La_{0.6}Sr_{0.4-x}Ti_xMnO_3$ (x=0.0-0.25) and $La_{1-x}Sr_xCoO_3$ (x=0.1-0.5); the reviewing of their crystal structures is also incorporated. The results showed the failure of the elastic bonding mechanism in all studied systems and revealed the general deficit of the valence charge in their unit cells. This valence deficit was not associated with the structural defects and was not equally localized in all coordination spheres. As the content of substitution increased, the charge deficit declined systematically from balanced level, signifying the transfer of valence charge from the $\tilde{O}_6$ to $\tilde{O}_{12}$ spheres. This transfer depended on the valence deviation of spheres and the average reached near 2 electron per unit cell. The possible impact of the limitted accuracy of the available structural data on the bond valence results has also been considered.

***Keywords***: Perovskite, Valence, Charge, Stoichiometry, Structure

## 1. Introduction

Many application significant properties of perovskites $ABO_3$ are believed to have origin in their structures. But despite its simplicity, the perovskite structures still pose many questions and among them the stoichiometry of elements. The common consensus is to consider a small diversity from the perfect formula and to write $ABO_{3-\delta}$ or $A_{1-\delta}B_{1-\delta}O_3$ instead of $ABO_3$ [25]. The always associates with the physical structure of materials and represents the missing mass of elements, to which the valence defects derive. In this paper we introduce a method to show that this diversity may arise purely from the valence distribution without any physical defects. The results for the exemplified systems revealed the asymmetric valence charge distribution and certain valence transfer between the coordination spheres of the metals.

The valence theory of chemical bond originated from L. Pauling when he postulated the so-called *valence principle* [2,3] which says that the atomic valence of any atom X is equal to the sum of valences of all bonds to X: $v = \sum v_i$. Evidently, this atomic valence is equivalent to the absolute value of oxidation state of the given atom (e.g. atom $\tilde{O}^{2-}$ has atomic valence of $v = |-2| = 2$). Similarly, the bond valence (BV) is equivalent to the number of bonding electrons (BE) distributed within the bond, for examples the average BE in the coordination sphere $[Co^{2+}\tilde{O}^{2-}_6]$ is 2/6 = 0.333 e per bond. The dependence of BV on bond length (BL) was subject of the extensive studies for decades [1,4-5,9,28-31] and many functional dependences were published, most of them

Manuscript Received: Jan. 31, 2015 / Revised: Feb. 5, 2015 / Accepted: Feb. 10, 2015
Corresponding Author: dinhchau@vnu.edu.vn
Tel: +84-4-3754-7461, Fax: +84-4-3754-7460
Faculty of Engineering Physics and Nanotechnology, VNU-University of Engineering and Technology, Vietnam

was summarized in [4]. All these functions are the exponential functions of general form $v_i=e^{(R_0-R)/B}$ where $R_0$ and $B$ are empirical parameters determined particularly for each donor-acceptor pair, usually for the metal-oxygen bonds (Fig.1). According to these relationships, when the BLs increase, the BVs must decrease and *vice versa*. This characteristic dependence was postulated by Brown in a principle called the *distortion theorem* which says: "*The product of BV and average BL is constant for the same bonds*" (i.e. $v_i \times \langle R_i \rangle = const$) [1]. Although this principle is not valid in general, it proves correct for many cases, especially for the ionic compounds. It is clear that this principle illustrates the elastic bonding mechanism: when the BLs vary, the BVs must

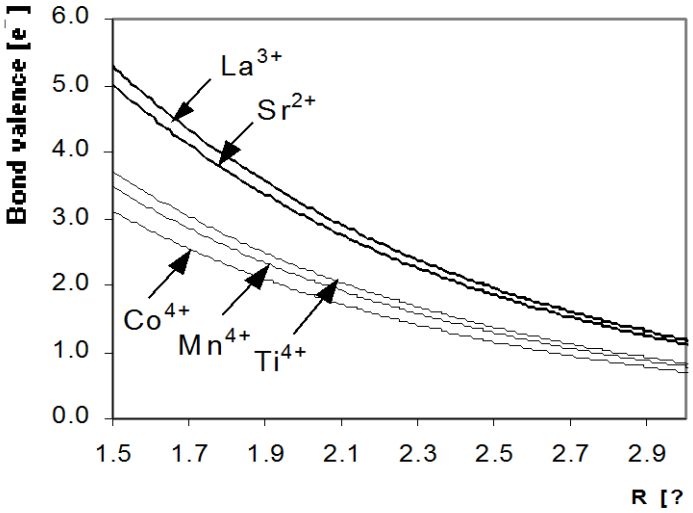


also change to preserve the electric neutrality of molecule and the stoichiometry of total atomic valence.

**Fig. 1. The bond valence curves for several cations**

The distortion theorem can be used, as we show here, to analyse the bonding properties of perovskites where the substitution of various elements (e.g. A=$La^{3+}$, $Sr^{2+}$, ...; B=$Mn^{3+}$, $Co^{3+}$...) of different oxidation states to the same lattice positions deforms the original cubic f-b-c lattice ($A^{3+}B^{3+}O_3^{2-}$). For the perovskites having atom X at lower oxidation state (e.g. $Sr^{2+}$) replacing atom A at higher oxidation state (e.g. $La^{3+}$) with *x%*, the common opinion is that some portion of atom B (e.g. $Co^{3+}$) must also change its oxidation state to higher (e.g. $Co^{4+}$). This consequently, as stated by distortion theorem, leads to the increase in the valences of bonds around atom B and to the shortening of the lattice constants connecting the atoms B. However, the experimental results, as discussed later, did not confirm the contract of lattices. For all studied perovskites, the lattice parameters changed only a little, reflecting no significant variation in bond valences, i.e. the number of electrons distributed within the unit cell remains unchanged. Thus the unit cell must be under-charged comparing to the state predicted by distortion theorem. This situation either forces the variation in stoichiometry of some atoms, namely of the oxygens if distortion theorem holds, or signifies the irregular charge relocation phenomenon within perovskite lattice if distortion theorem is considered as failed.

The bond valence method, however, requires knowledge of the interatomic distances which are not always available in the literature. To enable the use of this method for a larger group of perovskites we have developed a simple procedure for obtaining the bond valences directly from lattice parameters. In this paper we (a) review the crystal structures of the following perovskites: $La_{1-x}Pb_xMnO_3$ ($x$=0.1-0.5) and $La_{0.6}Sr_{0.4-x}Ti_xMnO_3$ ($x$=0.0-0.25) determined by the Rietveld method.; (b) present the theoretical concepts for obtaining bond valences and for estimation of non-stoichiometry parameter; (c) investigate the bond valence distribution and stoichiometry of several perovskite systems, including the two above, the $La_{1-x}Sr_xCoO_3$ (x=0.0-0.5) and five other systems, drawing attention to the failure of distortion theorem and finally (d) discuss the valence charge transfer between the coordination spheres of metals in perovskites and point to some possible consequences. Th

eoretical concepts are given in Section 2 and results are discussed in Section 3. Detailed discussion on failure of distorsion theorem and valence charge transfer phenomenon is found in the Sections 4 and 5. Section 6 pr ovides some remarks and conclusions are given in Section 7.

All samples had been prepared by the conventional solid-state reaction method. For $La_{1x}Pb_xMnO_3$: the ra w powders $La_2O_3$, PbO and $MnCO_3$ were presintered in air at $900^0$C-$1000^0$C for 15 hours then removed, regr ound and pressed into pellets and sintered at the same temperature for 15hours. For $La_{0.6}Sr_{0.4x}Ti_xMnO_3$: the r aw powders $La_2O_3$, $SrCO_3$, $TiO_2$, $MnCO_3$ were presintered in air at $1250^0$C for 10 hours and then sintered at $1300^0$C for 12 hours. The powder samples were measured at room temperature using the Bruker's X-Ray Dif fractometer D5005 at Center for Materials Science, Faculty of Physics, Hanoi University of Science. Step an gle 0.03, from $10^0$ to $70^0$, profile points 2000. Profiles were optimised using Pseudo-Voight functions. Lattice structures were determined by three methods: Ito [6], Visser [7] and Taupin [8]. Rietveld refinement was carried out using program MPROF [5].

## 2. Bond valence theory of perovskites

### 2.1. Perovskites in the 'pseudo-cubic' lattice

The oblique perovskite lattice is the cubic f-b-c with lattice constant $a \sim 3.8$ Å where atom A occupies ori gin A(0,0,0); B occupies b-c position B(½ ,½ ,½ ); and O occupies 3 f-c positions $O_1$(½ ,½ ,0), $O_2$(½ ,0,½ ), $O_3$(0, ½ ,½ ). These 3 f-c positions are equivalent only in the cubic lattice, not in lower symmetry. The coordination number of A is 12 $AO_{12}$, of B is 6 $\tilde{B}O_6$, of O is 2+4 ($\tilde{O}B_2A_4$) (**Fig.2**). The cubic lattice may be deformed to th e lower symmetries, e.g. to the monoclinic (*a=c≠b~3.8*Å , 90°, ~90°), or to the rhombohedral (*a=b=c~3.8*Å , ~90°; note that the frequently reported hexagonal lattice *a=b~5.5*Å and *c~6.6*Å or *c~13.0*Å , 90°, ı ˜ ° is equi valent to the rhombohedral one) or even to the triclinic lattice (*a≠b≠c~3.8*Å , ≠ ≠ 90). Some other lattice type s, such as tetragonal (a=b=c~7.6Å ), also exist.

Despite their variety, the perovskite lattices are usually centrosymmetric, so the inversion ˜1 can be consid ered. For this reason we call hereinafter the *pseudo-cubic* lattice the distorted cubic lattice (z=1) conserving t he site symmetry ˜1. The atoms in the pseudo-cubic lattice reside at the centrosymmetric positions. For cases where the atomic positions are not available, we transform the lattices to the pseudo-cubic form and derive th e bonding parameters directly from the lattice constants.

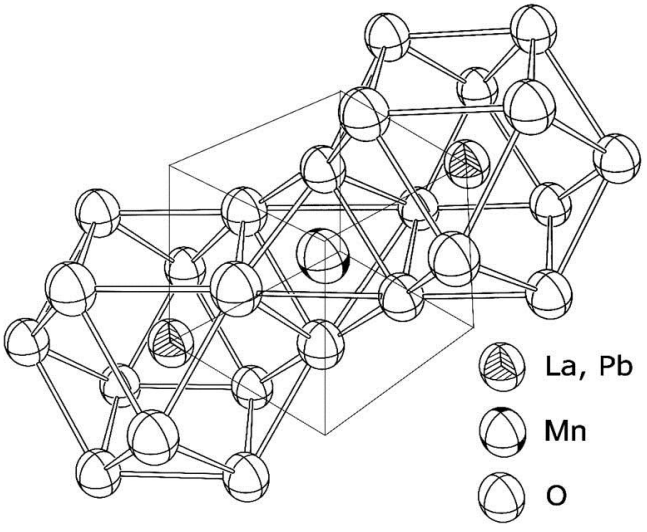


**Fig. 2 Stacking of coordination polyheders for ($La_{1-x}Pb_x$)$MnO_3$. The lines connecting the oxygens do not mean the bonds and are drawn only to shape the coordination polyeders**

### 2.2. Calculation of BV for pseudo-cubic cell

In general triclinic symmetry $P\bar{1}$ the coordination sphere $\tilde{A}O_{12}$ of atom A consists from 3 tetragons $A^{\cdots}O_4$; bonds within each tetragon are divided into 2 groups of equal length $\tilde{A}O$, so the $\tilde{A}O_{12}$ polyheder setup up 6 d ifferent bond lengths. The coordination sphere $\tilde{B}O_6$ consists from 3 pairs $B^{\cdots}O_2$ setting up 3 different bond le ngths. For oxygen, the coordination sphere $\tilde{O}B_2A_4$ consists from 1 pair $\tilde{O}B_2$ plus 2 pairs $\tilde{O}A_2$ setting up 3 diff erent bond lengths for each oxygen positions $O_1$(½ ,½ ,0), $O_2$(½ ,0,½ ), $O_3$(0,½ ,½ ). The bond valences may be d erived from the lattice constants as followed. Let $\vec{a}, \vec{b}, \vec{c}$ be the lattice vectors. By using Pauling's bond-vale nce sum rule $v = \sum v_i = \sum e^{(\tilde{R}o\tilde{R})/B}$ we obtain the following relations for triclinic symmetry:

(1) *Valence of A:* $v_A = v_{A1} + v_{A2} + v_{A3}$

$$v_{A1} = 2e^{(R_0 - |(\vec{a}+\vec{b})/2|)/B} + 2e^{(R_0 - |(-\vec{a}+\vec{b})/2|)/B}$$

$$v_{A2} = 2e^{(R_0 - |(\vec{a}+\vec{c})/2|)/B} + 2e^{(R_0 - |(-\vec{a}+\vec{c})/2|)/B}$$

$$v_{A3} = 2e^{(R_0 - |(\vec{c}+\vec{b})/2|)/B} + 2e^{(R_0 - |(-\vec{c}+\vec{b})/2|)/B}$$

(2) *Valence of B:* $v_B = v_{B1} + v_{B2} + v_{B3}$

$$v_{B1} = 2e^{(R_0 - |\vec{a}/2|)/B}; v_{B2} = 2e^{(R_0 - |\vec{b}/2|)/B}; v_{B3} = 2e^{(R_0 - |\vec{c}/2|)/B}$$

(3) *Valence of O:* There are 3 independent positions $O_1$, $O_2$ and $O_3$ so the valence is calculated for each case s eparately:

$v_{O1} = v_{\tilde{B}O1} + v_{\tilde{A}O1}$ ; $v_{O2} = v_{\tilde{B}O2} + v_{\tilde{A}O2}$ ; $v_{O3} = v_{\tilde{B}O3} + v_{\tilde{A}O3}$

$$v_{B-O_1} = 2e^{(R_0 - |\vec{a}/2|)/B}; v_{B-O_2} = 2e^{(R_0 - |\vec{b}/2|)/B}; v_{B-O_3} = 2e^{(R_0 - |\vec{c}/2|)/B}$$

$$v_{A-O_1} = 2e^{(R_0 - |(\vec{b}+\vec{c})/2|)/B} + 2e^{(R_0 - |(-\vec{b}+\vec{c})/2|)/B}$$

$$v_{A-O_2} = 2e^{(R_0 - |(\vec{a}+\vec{c})/2|)/B} + 2e^{(R_0 - |(-\vec{a}+\vec{c})/2|)/B}$$

$$v_{A-O_3} = 2e^{(R_0 - |(\vec{b}+\vec{a})/2|)/B} + 2e^{(R_0 - |(-\vec{b}+\vec{a})/2|)/B}$$

The average valence for atom O is:

$\langle v_O \rangle = (v_{O1} + v_{O2} + v_{O3}) / 3$

(4) *The electric neutrality of molecule requires*:

$v_A + v_B \; v_{O1} \; v_{O2} \; v_{O3} = 0$

This relation only means $v_A + v_B = v_{O1} \; v_{O2} \; v_{O3}$. It does not say $v_A + v_B = 3 \times |2| = 6$. In fact this sum ma y differ from 6 and this diversity signifies the real charge in the unit cell. The non-stoichiometry parameter is determined on the basis of this diversity.

Where there is an atom $X^{2+}$ replacing atom $A^{3+}$ with $x$% content, the valence spheres $A^{3+}O_{12}$ change to $A^{3+}O_{12}$ plus $X^{2+}O_{12}$ and the spheres $\tilde{O}A^{3+}{}_4$ change to $\tilde{O}A^{3+}{}_4$ plus $\tilde{O}X^{2+}{}_4$. Here we assume that the atoms X repla ce A homogeneously, that is all oxygen positions $O_1$, $O_2$ and $O_3$ contribute to the change of oxygen valence e qually. Let define the average valence $\langle v_A \rangle$ in the A-position as:

$\langle v_A \rangle = v_A \times (\tilde{1}x) + v_X \times x$ , where $v_X$ is calculated as for $v_A$ but with $R_0$ for $X^{2+}O$.

Evidently $\langle v_A \rangle$ decreases with increasing $x$ since the valence of X (2+) is lower than of A (3+). Therefore, the atoms B tend to compensate this charge deficiency by exhibiting both oxidation states 3+ and 4+. A porti on of $B^{3+}$ will move to $B^{4+}$. Suggest that this portion is equal to $x$%, the average valence at B positions is defi ned as followed:

$\langle v_B \rangle = v_{B+3} \times (1 \; x) + v_{B+4} \times x$ , where $v_{B+4}$ is calculated as for $v_{B+3}$ but with $R_0$ for $B^{4+}O$.

Similarly, for the calculation of oxygen valence $v_O = (v_{O1} + v_{O2} + v_{O3})/3$, the valences $v_{AO1}$, $v_{AO2}$, $v_{AO3}$ at $O_1$, $O_2$ and $O_3$ positions should be replaced by the averages $\langle v_{AO1}\rangle$, $\langle v_{AO2}\rangle$, $\langle v_{AO3}\rangle$ defined as:

$\langle v_{AO(i)}\rangle = v_{AO(i)} \times (1-x) + v_{XO(i)} \times x$, ($i$=1..3)

The $v_{XO1}$, $v_{XO2}$, $v_{XO3}$ are calculated as for $v_{AO1}$, $v_{AO2}$, $v_{AO3}$ but with the $R_0$ for bond $X^{2+}O$. Since the replacing of A by X splits B into 2 different oxidation states 3+ and 4+, we must also replace $v_{BO1}$, $v_{BO2}$, $v_{BO3}$ by their averages:

$\langle v_{BO(i)}\rangle = v_{B^{3+}O(i)} \times (1-x) + v_{B^{4+}O(i)} \times x$, ($i$=1..3)

**Table 1. Parameter $R_0$ for the studied compounds**

| *Bond* | $R_0$ | *Bond* | $R_0$ |
|---|---|---|---|
| $La^{3+}O$ | 2.172 | $Nd^{3+}O$ | 2.105 |
| $Sr^{2+}O$ | 2.118 | $Fe^{3+}O$ | 1.759 |
| $Co^{3+}O$ | 1.670 | $Na^{1+}O$ | 1.803 |
| $Co^{4+}O$ | 1.640 | $Eu^{3+}O$ | 2.074 |
| $Mn^{3+}O$ | 1.760 | $Ti^{4+}O$ | 1.815 |
| $Mn^{4+}O$ | 1.753 | $Pb^{2+}O$ | 2.112 |

For the parameters $R_0$ in the above relations, Table 1 summarizes all used values. They are taken from [4]. The parameter B is set fixed at 0.370 for all cases. The above discussed formalism is limitted to the substitution of the element $X^{2+}$ for $A^{3+}$ in A-positions (0,0,0). The possibility of $X^{2+}$ replacing $B^{3+}$ at (½ ,½ ,½ ), or even replacing $O_1$, $O_2$, $O_3$ at (½ ,½ ,0), (½ ,0,½ ) and (0,½ ,½ ) is not considered.

## 3. The structural data

### 3.1. The pseudo-cubic lattices

The pseudo-cubic lattices of the studied systems have been obtained by Rietveld refienement.

(a) For $La_{1x}Pb_xMnO_3$ (x=0.1-0.5) the refinement was successful in the pseudo-cubic lattices with the symmetry decreased from cubic (x=0.5) to rhombohedral (x=0.4) and triclinic (x=0.3, 0.2, 0.1). The results are summarized in **Table 2** with the standard deviations given in the parenthesis. For x= 0.4-0.5 all atomic positions were fixed; for x =0.1-0.3 the metals positions were fixed while the oxygens were refined. The existence of a cubic cell for x=0.5 is very similar to of compounds $La_{1-x}Sr_xCoO_3$ [17,18]. The variation of unit cell volumes was V/V=1.0% i.e. max-min variation=0.6Å $^3$. The largest volume occurred for x=0.2, 0.3 and the smallest for x=0.5. The diversity in lattice constants is 0.5% (from 3.877 to 3.895Å ). **Table 3** shows bond lengths and bond angles for MnO and OMnO. The average MnOMn angle increases with *x* and reaches maximum for *x=0.4* and *0.5* whereas the length MnO decreases continuously to the minimum for *x=0.5*.

**Table 2. Atomic postions, B and s.o.f. for $La_{1-x}Pb_xMnO_3$**

| *x* | *Atom* | *x* | *y* | *z* | *B* | *s.o.f.* | *S.G. a,b,c . . .* | $R_I$ $R_P$ *V* |
|---|---|---|---|---|---|---|---|---|
| 0.1 | Pb | 0.0 | 0.0 | 0.0 | 0.24 | 0.11 | P1 | 6.2 |
| | La | 0.0 | 0.0 | 0.0 | 0.29 | 0.89 | 3.880(2) | 11.6 |
| | $Mn^{3+}$ | 0.5 | 0.5 | 0.5 | 0.39 | 0.73 | 3.882(1) | 58.6 |
| | $Mn^{4+}$ | 0.5 | 0.5 | 0.5 | 0.39 | 0.27 | 3.890(1) | |
| | O1 | 0.431(2) | 0.500(1) | 0.000 | 1.40 | 0.98 | 90.56(3) | |
| | O2 | 0.500(2) | 0.000 | 0.406(8) | 1.40 | 0.98 | 90.37(3) | |
| | O3 | 0.000 | 0.422(1) | 0.500(4) | 1.40 | 0.98 | 90.54(1) | |
| 0.2 | Pb | 0.0 | 0.0 | 0.0 | 0.24 | 0.21 | P1 | 4.9 |
| | La | 0.0 | 0.0 | 0.0 | 0.29 | 0.81 | 3.887(5) | 10.5 |
| | $Mn^{3+}$ | 0.5 | 0.5 | 0.5 | 0.29 | 0.76 | 3.894(1) | 58.9 |
| | $Mn^{4+}$ | 0.5 | 0.5 | 0.5 | 0.29 | 0.20 | 3.893(1) | |

| | | | | | | | | |
|---|---|---|---|---|---|---|---|---|
| | O1 | 0.545(1) | 0.416(4) | -0.001(4) | 1.45 | 1.00 | 90.38(2) | |
| | O2 | 0.481(3) | 0.001(7) | 0.418(5) | 1.45 | 1.00 | 90.42(3) | |
| | O3 | 0.000 | 0.474(4) | 0.450(1) | 1.45 | 1.00 | 90.41(5) | |
| | Pb | 0.0 | 0.0 | 0.0 | 0.40 | 0.29 | P1 | 2.8 |
| | La | 0.0 | 0.0 | 0.0 | 0.33 | 0.69 | 3.895(4) | 10.2 |
| | $Mn^{3+}$ | 0.5 | 0.5 | 0.5 | 0.36 | 0.77 | 3.891(1) | 58.9 |
| 0.3 | $Mn^{4+}$ | 0.5 | 0.5 | 0.5 | 0.36 | 0.21 | 3.882(1) | |
| | O1 | 0.424(6) | 0.493(1) | 0.000 | 1.35 | 0.97 | 90.28(1) | |
| | O2 | 0.568(1) | .000 | 0.507(7) | 1.35 | 0.97 | 90.40(2) | |
| | O3 | -0.004(7) | 0.469(7) | 0.533(5) | 1.35 | 0.97 | 90.37(1) | |
| | Pb | 0.0 | 0.0 | 0.0 | 0.40 | 0.38 | Rhombo | 2.5 |
| | La | 0.0 | 0.0 | 0.0 | 0.53 | 0.64 | $R\bar{3}c$ | 9.3 |
| | $Mn^{3+}$ | 0.5 | 0.5 | 0.5 | 0.71 | 0.78 | 3.885(1) | 58.64 |
| 0.4 | $Mn^{4+}$ | 0.5 | 0.5 | 0.5 | 0.86 | 0.20 | 90.05(5) | |
| | O1 | 0.5 | 0.5 | 0.0 | 1.06 | 1.00 | | |
| | O2 | 0.5 | 0.0 | 0.5 | 1.06 | 1.00 | | |
| | O3 | 0.0 | 0.5 | 0.5 | 1.06 | 1.00 | | |
| | Pb | 0.0 | 0.0 | 0.0 | 0.40 | 0.48 | Cubic | 2.3 |
| | La | 0.0 | 0.0 | 0.0 | 0.53 | 0.53 | Pm3m | 8.4 |
| | $Mn^{3+}$ | 0.5 | 0.5 | 0.5 | 0.71 | 0.79 | 3.877(4) | 58.3 |
| 0.5 | $Mn^{4+}$ | 0.5 | 0.5 | 0.5 | 0.86 | 0.18 | 90 | |
| | O1 | 0.5 | 0.5 | 0.0 | 1.06 | 3.01 | | |

The $La_{1x}Pb_xMnO_3$ compounds, known to be the feromagnetic materials, have been investigated in [20,21]. Rec ent interest on these compounds [19,22] was due mainly to the colossal magnetoresistance effect (CMR) discover ed in the $Ln_{\tilde{1}x}A_xMnO_3$ ($Ln^{3+}$ = trivalent rare-earth, A= divalent metals $Ca^{+2}$, $Sr^{2+}$, $Ba^{2+}$, $Pb^{2+}$) (see e.g. [23]).

In [22] the Rietveld analysis was done for all *x*=0.0-0.5 in the hexagonal space group $R\bar{3}c$. To compare these r esults with ours, the pseudo-cubic lattices should be transformed by the transformation matrix [(1,1,0) (0,$\tilde{1}$,1) (2,2, 2)]. Except for *x*=0.1 and 0.2 where small angular deformations were seen by our samples (<$0.2^0$) all other cases d iffered only in the cell constants. By average their cells are 0.5% smaller i.e. 0.3Å $^3$/unit cell. The increment of M$\tilde{n}$ $\tilde{O}$Mn angles due to substitution was also lesser than in our samples.

**Table. 3 Bond lengths [Å] and bond angles [$^0$] for $La_{1\ \ x}Pb_xMnO_3$**

| *x* | *to* | *Mn̂O* | *Mn̂ÕMn* | *x* | *Mn̂O* | *Mn̂ÕMn* |
|---|---|---|---|---|---|---|
| | $O_1$ | 1.962, 1.965 | 164.3 | | 1.964, 1.971 | 162.6 |
| *0.1* | $O_2$ | 1.972, 1.979 | 158.7 | *0.3* | 1.960, 1.966 | 164.5 |
| | $O_3$ | 1.961, 1.966 | 162.3 | | 1.937, 1.974 | 169.7 |
| | $O_1$ | 1.979, 1.984 | 158.5 | *0.4* | 1.943 | 180.0 |
| *0.2* | $O_2$ | 1.967, 1.979 | 161.0 | *0.5* | 1.939 | 180.0 |
| | $O_3$ | 1.956, 1.956 | 166.9 | | | |

(*b*) $La_{0.6}Sr_{0.4-x}Ti_xMnO_3$. These structures are very common to of doped lanthanum manganates, although the fo rmula stoichiometry does not argue for such conclusion. It seems that mixing of raw materials according to the giv en stoichiometry would questionably lead to the replacement of (La, Sr) by $Ti^{4+}$ since the ionic radius of $Ti^{4+}$ (0.42 Å , original $TiO_2$) is much smaller than of $La^{3+}$ and $Sr^{2+}$ (1.032Å , 1.18Å ) and is comparable to of $Mn^{3+}$, $Mn^{4+}$ (0.58 Å , 0.39Å ) [26]. The $Ti^{4+}$ fit naturally better into the ($Mn^{3+}$, $Mn^{4+}$) positions.

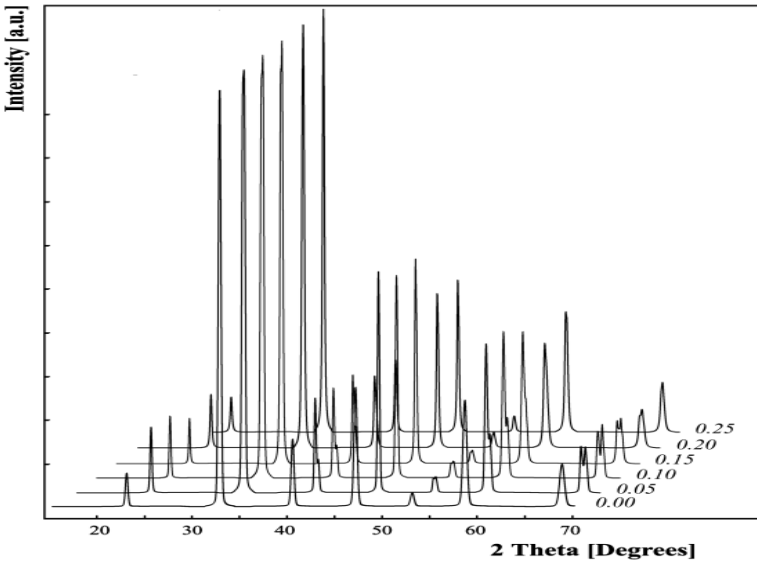


**Fig. 3. X-Ray diffraction patterns of $La_{0.6}Sr_{0.4-x}Ti_xMnO_3$.**

However, the X-Ray diffraction patterns (Fig.3) showed the common peak positions for perovskites, revealing directly the lengths of possible crystallographic axis.

**Table 4. Thermal parameter B and s.o.f. for $La_{0.6}Sr_{0.4-x}Ti_xMnO_3$**

| *x* | *Atom* | *B* | *s.o.f.* | *S.G.* *a*, , *V* $R_I$ ,$R_P$ | *x* | *B* | *s.o.f.* | *S.G.* *a*, , *V* $R_I$ ,$R_P$ |
|---|---|---|---|---|---|---|---|---|
| | La | 0.41 | 0.60 | Rhombo | | 0.30 | 0.59 | Rhombo R $\bar{3}$ c |
| | Sr | 0.77 | 0.40 | R $\bar{3}$ c | | 0.80 | 0.25 | 3.908(1) |
| | Ti | 0.00 | 0.00 | 3.880(3) | | 0.53 | 0.15 | 90.3(1) |
| 0.00 | $Mn^{3+}$ | 0.30 | 0.72 | 90.1(2) | 0.15 | 0.22 | 0.55 | 59.7 |
| | $Mn^{4+}$ | 0.30 | 0.32 | 58.4 | | 0.22 | 0.45 | 5.2 |
| | O1 | 1.22 | 0.97 | 3.9 | | 2.38 | 1.01 | 11.4 |
| | O2 | 1.22 | 0.97 | 12.7 | | 2.38 | 1.01 | |
| | O3 | 1.22 | 0.97 | | | 2.38 | 1.01 | |
| | La | 0.51 | 0.62 | Rhombo | | 0.57 | 0.61 | Rhombo R $\bar{3}$ c |
| | Sr | 0.85 | 0.35 | R $\bar{3}$ c | | 0.86 | 0.19 | 3.905(1) 90.2 |
| | Ti | 0.57 | 0.05 | 3.889(2) | | 0.60 | 0.19 | (2) |
| 0.05 | $Mn^{3+}$ | 0.30 | 0.71 | 90.3(3) | 0.20 | 0.48 | 0.57 | 59.5 |
| | $Mn^{4+}$ | 0.30 | 0.31 | 58.8 | | 0.48 | 0.43 | 4.8 |
| | O1 | 1.34 | 1.00 | 6.4 | | 1.42 | 0.98 | 11.9 |
| | O2 | 1.34 | 1.00 | 11.7 | | 1.42 | 0.98 | |
| | O3 | 1.34 | 1.00 | | | 1.42 | 0.98 | |
| | La | 0.49 | 0.63 | Rhombo | | 0.27 | 0.60 | Rhombo R $\bar{3}$ c |
| | Sr | 0.31 | 0.30 | R $\bar{3}$ c | | 0.54 | 0.16 | 3.900(3) |
| | Ti | 0.23 | 0.10 | 3.902(5) | | 0.59 | 0.27 | 90.1(1) |
| 0.10 | $Mn^{3+}$ | 0.29 | 0.61 | 90.3(5) | 0.25 | 0.38 | 0.53 | 59.3 |
| | $Mn^{4+}$ | 0.17 | 0.38 | 59.4 | | 0.38 | 0.47 | 6.8 |
| | O1 | 1.72 | 0.98 | 5.9 | | 1.63 | 1.00 | 13.8 |
| | O2 | 1.72 | 0.98 | 12.9 | | 1.63 | 1.00 | |
| | O3 | 1.72 | 0.98 | | | 1.63 | 1.00 | |

All structures were refinable in the rhombohedral space group R $\bar{3}$ c with the atomic positions set fixed. Table 4 lists the results. The replacement of $Mn^{4+}/Mn^{3+}$ by the $Ti^{4+}$ was not observed (zeroed s.o.f.). The occurence of $Ti^{2+}$ and/or $Ti^{3+}$ was not also seen.

The max-min diversity of lattice constants is 0.7%, i.e. 0.03Å and of volumes is 2%, i.e. 1.3Å $^3$. The mean vol ume <V>=59.2Å $^3$. The average (La, Sr, Ti)O distances, as deduced from the lattice constants are: 2.744, 2.750, 2. 759, 2.764, 2.761, 2.758Å for *x* =0.00.25 sequentially. Similarly, the bond lengths MnO are: 1.940, 1.945, 1.9

51, 1.954, 1.953, 1.950Å . The maximal values occur for $x$=0.15. The bond angles MnÕMn holds fixed at 180 $^{o}$ for all samples.

(*c*) $La_{1x}Sr_xCoO$ . Here the pseudo-cubic lattices were obtained by transformation of various known structures. For cases where reflection lists were available [15,16] we have re-calculated the lattice parameters and refined them in the pseudo-cubic form. Some differences occured, mostly for the structures published earlier e. g. $La_{0.6}Sr_{0.4}CoO$ [15], $La_{0.5}Sr_{0.5}CoO$ $La_{0.9}Sr_{0.1}CoO$ [16]. Commonly, the transformed lattices agree well with each other (max-min diversity of lattice constants is less than 0.4%, i.e. <0.01Å ). A general conclusion can be made as followed. For $x$ =0.0-0.5 the step-by-step changing of the lattice constants from 3.830Å to 3.836 Å was observed but was not significant. With respect to those small changes the pseudo-cubic lattices of $La_{1x}Sr_xCoO$ should be regarded as solid, more-less independent to the substitution of $Sr^{2+}$. This is well reflected in the almost constant unit cell volume at all $x$ (mean <V>=56.3(2)Å $^{3}$).

**Table 5. The pseudo-cubic lattices of $La_{1\ x}Sr_xCoO_3$**

| *x* | *Cell* | *a* [Å], [º] | *V* [Å $^{3}$] | *Ref.* |
|---|---|---|---|---|
| 0.00 | Rhombo | 3.826(2), ~ . ! | 56.0(3) | [17] |
| 0.10 | Rhombo | 3.832(3), ~ . . | 56.3(2) | [15,17] |
| 0.20 | Rhombo | 3.836(2), ~ . ! | 56.5(1) | [15,17] |
| 0.25 | Orthorh. | 3.831(6), 3.844(8), 3.840(1), 90 | 56.5(3) | [18] |
| 0.30 | Rhombo | 3.834(1), ~ . ! | 56.3(1) | [16,17] |
| 0.35 | Rhombo | 3.832(3), ~ . . | 56.3(1) | [18] |
| 0.40 | Rhombo | 3.831(1), ~ . . | 56.2(2) | [15,17] |
| 0.45 | Rhombo | 3.830(4), ~ . . | 56.2(2) | [18] |
| 0.50 | Cubic | 3.832(1), ~ | 56.3(2) | [16] |

It is worth to notice here that such conclusion is radically different from the common view where the trend is to confirm the influence of substitution on the change of lattice parameters. In solid state physics, the usual practice is to associate phenomena with some phase transition or structural change and the above conclusion is not favourite. Next table summaries results and references.

With respect to the small variations in the lattice constants, the deduced atomic distances vary only a little: from 1.913 to 1.922Å for CoO and from 2.689 to 2.722Å for (La, Sr)O. Visibly, there is more change on (La, Sr)O. The $CoO_6$ coordination spheres can be decribed as regular, rigid and almost non-distorted. The angles CoÕCo are 180$^{o}$ for all samples.

### 3.2. Bond valence and non-stoichiometry

In Table 6 the atomic bond valences for the given perovskites are shown. Where the atomic positions and interatomic distances are available the BVs were obtained by inserting the bond lengths directly into the formula $v_i=e^{(R_0-R)/B}$. For the other cases, the procedure 2.2. applied. The total bonding electrons in one molecule (i.e. in the asymmetric unit of the pseudo-cubic unit cell) is equal to the total positive charges communicated by all positive cations *BE* . $<v_A>$ $<v_B>$. Consequently, the expected oxygen stoichiometry is $n$(O) = *BE* /2. The non-stoichiometry parameter is calculated as =3$n$(O). This directly associates with the valence charge and should correctly be stated as the *valence non-stoichiometry*. The measures by itself the *valence charge deficit* in the unit cell. The predicted cell constants $a$ (assuming rhombohedral case) satisfying condition =0, are listed in the last column. These values developed monotonuously with $x$ and differed radically from the measured cell constants. The detailed discussion on this topic is given in *Section 4.1*.

**Table 6. Bond valences and non-stoichiometry parameter. The shading values were calculated using results from Rietveld analysis, other ones were determined from pseudo-cubic lattice constants.**

| | *x* | $<v_A>$ | | $<v_B>$ | | | | *Meas.* $<a>$ | *Predic.* $a$ ( =0) |
|---|---|---|---|---|---|---|---|---|---|
| $La_{1x}Pb_xMnO_3$ | 0.1 | 2.22 | 2.44 | 3.63 | 3.42 | 0.08 | 0.14 | 3.879 | 3.863 |
| | 0.2 | 2.23 | 2.38 | 3.61 | 3.39 | 0.08 | 0.24 | 3.886 | 3.868 |
| | 0.3 | 2.27 | 2.36 | 3.61 | 3.46 | 0.06 | 0.19 | 3.885 | 3.873 |
| | 0.4 | 2.31 | 2.38 | 3.62 | 3.63 | 0.03 | -0.02 | 3.885 | 3.878 |

| | | | | | | | | |
|---|---|---|---|---|---|---|---|---|
| | 0.5 | 2.38 | 2.38 | 3.67 | 3.66 | -0.03 | -0.04 | 3.877 | 3.882 |
| $La_{0.6}Sr_{0.4-x}Ti_xMnO_3$ | 0.0 | 2.42 | | 3.66 | | -0.04 | | 3.880 | 3.889 |
| | 0.05 | 2.32 | | 3.62 | | 0.03 | | 3.889 | 3.883 |
| | 0.10 | 2.20 | | 3.57 | | 0.11 | | 3.902 | 3.877 |
| | 0.15 | 2.12 | | 3.55 | | 0.17 | | 3.908 | 3.871 |
| | 0.20 | 2.07 | | 3.57 | | 0.18 | | 3.905 | 3.865 |
| | 0.25 | 2.03 | | 3.58 | | 0.19 | | 3.900 | 3.858 |
| $La_{1-x}Sr_xCoO_3$ | 0.0 | 2.84 | | 3.11 | | 0.02 | | 3.826 | 3.821 |
| | 0.10 | 2.77 | | 3.06 | | 0.08 | | 3.832 | 3.814 |
| | 0.20 | 2.71 | | 3.02 | | 0.13 | | 3.836 | 3.808 |
| | 0.25 | 2.68 | | 3.00 | | 0.16 | | 3.831 | 3.804 |
| | 0.30 | 2.68 | | 3.01 | | 0.16 | | 3.834 | 3.801 |
| | 0.35 | 2.67 | | 3.00 | | 0.16 | | 3.832 | 3.798 |
| | 0.40 | 2.66 | | 2.99 | | 0.17 | | 3.831 | 3.794 |
| | 0.45 | 2.65 | | 2.99 | | 0.18 | | 3.830 | 3.791 |
| | 0.50 | 2.62 | | 2.97 | | 0.21 | | 3.832 | 3.787 |

For $La_{1x}Sr_xCoO_3$ and $La_{0.6}Sr_{0.\tilde{4}x}Ti_xMnO_3$ the increased with substitution but for $La_{\tilde{1}x}Pb_xMnO_3$ it decreased. Since for most cases >0, the unit cells would contain a bit less valence charge than 6. There are several ex ceptions with <0 near the boundary $x$=0.0 and 0.5. In general the charge deficit could happen by mean of t he physical presence of either metals or oxygen vacancies in the lattice. Our mechanism showed inversely th at it is principally normal in the real bonding spheres that the atomic valence must not be equal to the atomic stoichiometry.

In our samples the substitution seems to have the stronger effect on the change of the average valence at A-position $\langle v_A \rangle$ than at B-position $\langle v_B \rangle$. The $\langle v_A \rangle$ varied usually ~ 2 times more then the $\langle v_B \rangle$, i.e. $\langle v_A \rangle$/ $\langle v_B \rangle$=0.22/0.14 for $La_{\tilde{1}x}Sr_xCoO_3$; =0.39/0.09 for $La_{0.6}Sr_xTi_{0.\tilde{4}x}MnO_3$. The diverged values were found for L $a_{\tilde{1}x}Pb_xMnO_3$: 0.16/0.04 (from lattice) versus 0.06/0.24 (from Rietveld). This forces consideration that the val ence charge flows must more for the $\tilde{A}O_{12}$ corrdination spheres. Fig. 4 draws the ratio $\langle a \rangle/\langle v_A \rangle$ between the average measured cell constants $\langle a \rangle$ and the average valences at A-positions $\langle v_A \rangle$ against the non-stoichio metry parameter for the studied compounds. The dependence is almost linear (correlation coeficient squar e $R^2$>0.98). For dependence $=f(x)$ (see Fig. 5) the observed values did not show clear linear relationship.

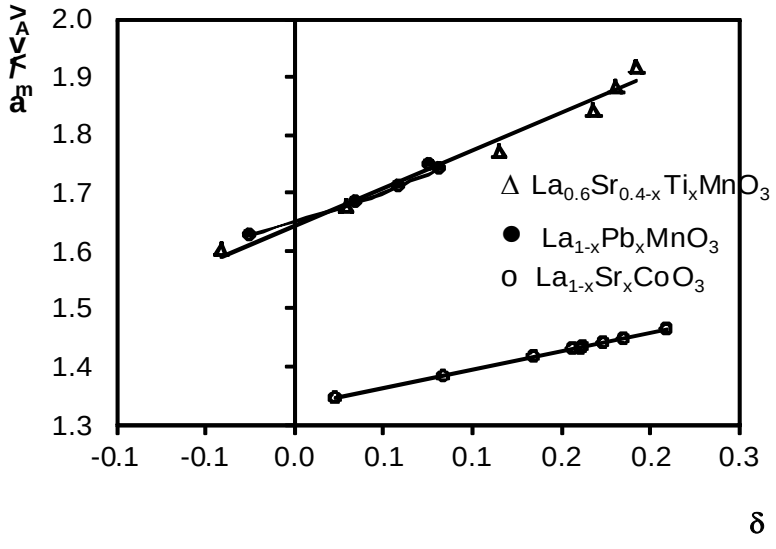


**Fig. 4. The linear relationship between $\langle a \rangle/\langle v_A \rangle$ and**

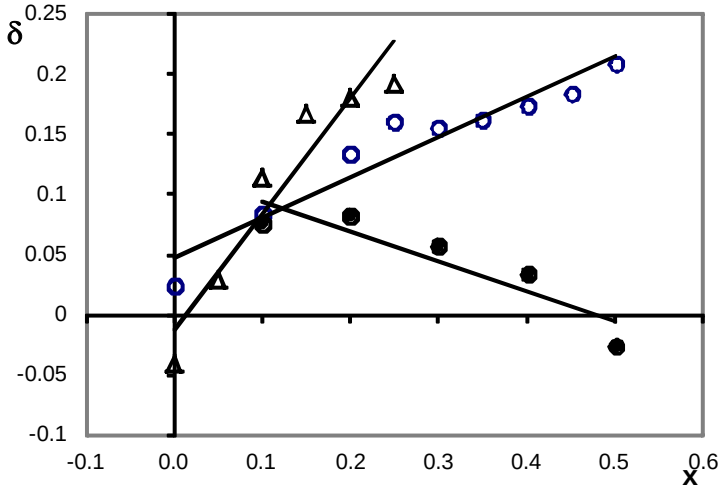


**Fig. 5. The non-linear dependence of on x for the studied perovskites. The legends are same as in Fig.4.**

## 4. Failure of distortion theorem

### 4.1. The development of lattice constants

Fig. 6 compares the predicted and the measured pseudo-cubic lattice constants for the studied compounds. As distortion theorem predicts, when bond length decreases the number of electrons communicated within th e bonds must increase. So the lattice tends to compensate unit cell charge deficiency by contracting the lattic e constants (inversely, the lattice should expand to reduce charge excess). The measured lattice constants sho wed, however, no such contraction.

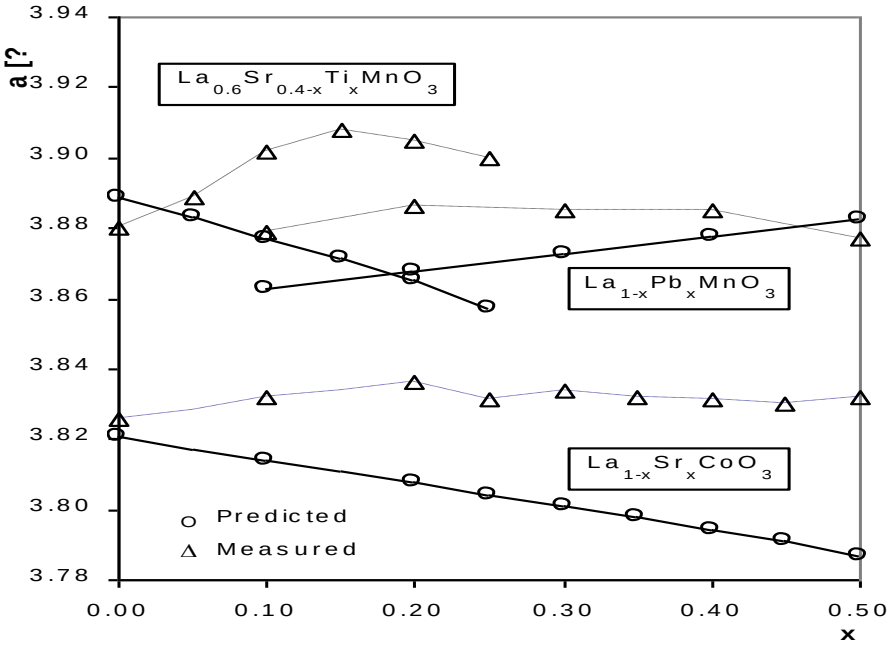


**Fig. 6. The predicted lattice constants versus the measured ones. The lines are drawn to guide the eyes.**

The rigidity of the coordination spheres may be expected for $CoO_6$ but not for $MnO_6$ (which is known to b e more elastic to Jahn-Teller effect). It seems that the factors which determine the structures are not what dri ve the valence charges. This incompatibility between the structure and the bonding ability should be seen as t he fundamental reason for a non-trivial distribution of the valence charge among the coordination spheres in perovskites.

As seen from Fig. 6, the maximal differences between measured and calculated lattice constants are 0.05 Å for $La_{0.6}Sr_{0.4-x}Ti_xMnO_3$, $La_{1-x}Sr_xCoO_3$ and 0.02Å for $La_{1-x}Pb_xMnO_3$. Since the lattice parameters are usually determined with accuracy of third decimal digit, these differences are quite significant. Until they did not dec rease below 0.01Å , they should be considered as significant differences. The smallest discrepancy for $La_{1-x}Pb_xMnO_3$ agrees well with a smaller change in the average valence $<v_A>$ and for this system. To clasify in te rms of the bond valences, the $La_{1-x}Pb_xMnO_3$ can be said to have the least irregular valence charge structure co mpared to the rest two compound systems. The charge deficit, as represented by , is ~0.1 e/u (electron/unit cell) for $La_{1-x}Pb_xMnO_3$ while it is ~0.2 e/u for the rests.

### 4.2. Test for the failure of distortion theorem in other perovskite systems

The validity of distortion theorem was tested for some other perovskite systems. The calculations were pe rformed using the published lattice data and the results are listed in Table 7.

**Table 7. Maximal difference between the calculated and the measur ed lattice constant (a), maximal valences $<v_A>$,$<v_B>$, maximal and t he x range for some perovskites**

| *Compound* | *a* | $<v_A>$ | $<v_B>$ | | *x range* | *Ref.* |
|---|---|---|---|---|---|---|
| $La_{1-x}Na_xMnO_3$ | 0.04 | 2.12 | 3.72 | 0.04 | 0.1-0.5 | 12 |
| $Ln_{0.8}Sr_{0.2}(Co_{1-x}Fe_x)O_3$ | 0.02 | 2.70 | 3.40 | 0.05 | 0.03-0.12 | 14 |
| $La_{0.5-x}Sr_{0.5-x}Fe_{0.4}Ti_{0.6}O_3$ | 0.07 | 2.62 | 3.64 | 0.07 | 0.0-0.10 | 13 |
| $Nd_{0.67}Sr_{0.33}Mn_{1-x}Fe_xO_3$ | 0.05 | 2.48 | 3.76 | 0.04 | 0.0-0.15 | 31 |
| $CoMnO_3$ | 0.08 | 1.96 | 4.46 | -0.17 | 0.0-0.05 | 24 |

For some cases the procedure 2.2 must be modified. Several conclusions can be made for the studied case s: (*a*) for none of the studied samples, the maximal | | has decreased below 0.01Å; (*b*) all samples showed t he diversity between observed and calculated lattice constants according to the content of substitution *x* but t he measure of diversity differed from case to case; (*c*) for most cases, the change of $<v_B>$ was smaller than of $<v_A>$, i.e. the A-positions have located more valence charge than the B-positions.

## 5. Valence charge distribution

### 5.1. Saturated bond length

There always exists for any oxidation state *v*, calculated as $v = \sum_{i=1}^{n} e^{(R_0 - R_i)/B}$ where *i* runs through all *n* bon ds in the coordination sphere, the average bond length $R_s$ specifying $v = ne^{(R_0 - R_s)/B}$. This $R_s$ is called hereinaf ter a *saturated bond length* for the given pair $R_0$, *B*. Evidently, $R_s = R_0 - B\log(v/n)$. With respect to the coord ination spheres $\tilde{A}O_{12}$ and $\tilde{B}O_6$ the saturated bond lengths $R_s(\tilde{A}O_{12})$ and $R_s(\tilde{B}O_6)$ set the demarcation line belo w which the coordination sphere become saturated, i.e. over-charged. Conversely, one should consider the va lence charge deficit in the coordination sphere if the larger average bond distances were systematically obser ved.

**Table 8. Some saturated bond lengths for bonding to oxygen**

| *Cation* | $\tilde{A}O_{12}$ | $\tilde{B}O_6$ | *Cation* | $\tilde{A}O_{12}$ | $\tilde{B}O_6$ |
|---|---|---|---|---|---|
| $Ba^{2+}$ | 2.948 | 2.691 | $Cu^{1+}$ | 2.519 | 2.263 |
| $Sr^{2+}$ | 2.781 | 2.524 | $Cu^{3+}$ | 2.252 | 1.995 |
| $Pb^{2+}$ | 2.775 | 2.518 | $Mn^{2+}$ | 2.453 | 2.196 |

| | | | | | |
|---|---|---|---|---|---|
| $Ag^{1+}$ | 2.761 | 2.505 | $Mn^{3+}$ | 2.273 | 2.016 |
| $Na^{1+}$ | 2.722 | 2.466 | $Mn^{4+}$ | 2.159 | 1.903 |
| $La^{3+}$ | 2.685 | 2.428 | $Co^{3+}$ | 2.183 | 1.926 |
| $Pr^{3+}$ | 2.651 | 2.394 | $Co^{4+}$ | 2.046 | 1.790 |
| $Hg^{2+}$ | 2.635 | 2.378 | $Pb^{4+}$ | 2.448 | 2.192 |
| $Ca^{2+}$ | 2.630 | 2.373 | $Ti^{4+}$ | 2.221 | 1.965 |
| $Nd^{3+}$ | 2.618 | 2.361 | $Fe^{2+}$ | 2.397 | 2.140 |
| $K^{1+}$ | 3.051 | 2.795 | $Cr^{6+}$ | 2.050 | 1.794 |
| $Er^{3+}$ | 2.501 | 2.244 | $Fe^{3+}$ | 2.272 | 2.015 |
| $Eu^{3+}$ | 2.587 | 2.330 | $Fe^{4+}$ | 2.186 | 1.930 |

Table 8 summaries the saturated bond lengths for several metals frequently encountered in perovskites an d Table 9 compares the measured bond distances with the calculated saturated bond lengths for the studied sy stems. According to Table 8, the cations listed in the left part of the table can hardly occupy B-positions sinc e their saturated bong lengths are much larger than the average bond lengths observed for the $\tilde{B}O_6$ spheres. If this would happen, these spheres would become heavily saturated. Similarly, if the cations listed in the right part of the table occur in $\tilde{A}O_{12}$ spheres then the resulting coordinations must be much non-saturated because t he listed saturated bond lengths are significantly smaller than the observed average bond lengths for these sp heres.

**Table 9. The average bond lengths and the saturated ones in the spheres A $O_{12}$ and B $O_6$ for the studied perovskites**

| | *x* | $\tilde{A}O_{12}$ *Meas.* | $\tilde{A}O_{12}$ *Satur.* | $\tilde{M}S$ | $\tilde{B}O_6$ *Meas.* | $\tilde{B}O_6$ *Satur.* | $\tilde{M}S$ |
|---|---|---|---|---|---|---|---|
| $La_{1-x}Pb_xMnO_3$ | 0.1 | 2.756 | 2.694 | 0.062 | 1.967 | 2.005 | -0.038 |
| | 0.2 | 2.760 | 2.703 | 0.057 | 1.970 | 1.994 | -0.024 |
| | 0.3 | 2.757 | 2.712 | 0.045 | 1.962 | 1.982 | -0.020 |
| | 0.4 | 2.747 | 2.721 | 0.026 | 1.943 | 1.971 | -0.028 |
| | 0.5 | 2.742 | 2.730 | 0.012 | 1.939 | 1.960 | -0.021 |
| $La_{0.6}Sr_{0.4-x}Ti_xMnO_3$ | 0.00 | 2.744 | 2.723 | 0.021 | 1.940 | 1.971 | -0.031 |
| | 0.05 | 2.750 | 2.695 | 0.055 | 1.945 | 1.982 | -0.037 |
| | 0.10 | 2.759 | 2.667 | 0.092 | 1.951 | 1.994 | -0.043 |
| | 0.15 | 2.763 | 2.639 | 0.124 | 1.954 | 2.005 | -0.051 |
| | 0.20 | 2.761 | 2.611 | 0.150 | 1.952 | 2.016 | -0.064 |
| | 0.25 | 2.757 | 2.583 | 0.174 | 1.950 | 2.028 | -0.078 |
| $La_{1-x}Sr_xCoO_3$ | 0.00 | 2.706 | 2.685 | 0.021 | 1.913 | 1.926 | -0.013 |
| | 0.10 | 2.710 | 2.695 | 0.015 | 1.916 | 1.913 | 0.003 |
| | 0.20 | 2.713 | 2.704 | 0.009 | 1.918 | 1.899 | 0.019 |
| | 0.25 | 2.714 | 2.709 | 0.005 | 1.919 | 1.892 | 0.027 |
| | 0.30 | 2.711 | 2.714 | -0.003 | 1.917 | 1.886 | 0.031 |
| | 0.35 | 2.710 | 2.719 | -0.009 | 1.916 | 1.879 | 0.037 |
| | 0.40 | 2.709 | 2.723 | -0.014 | 1.916 | 1.872 | 0.044 |
| | 0.45 | 2.708 | 2.728 | -0.020 | 1.915 | 1.865 | 0.050 |
| | 0.50 | 2.710 | 2.733 | -0.023 | 1.916 | 1.858 | 0.058 |

The data given in Table 9 reveal that the valence charge does not locate symmetrically on $\tilde{A}O_{12}$ and $\tilde{B}O_6$. Particularly, for $La_{0.6}Sr_{0.4-x}Ti_xMnO_3$ and $La_{1-x}Pb_xMnO_3$ the $\tilde{M}nO_6$ spheres are over-charged, whereas the (La,S r,Ti)$\tilde{O}_{12}$ and (La,Pb)$\tilde{O}_{12}$ spheres are under-charged. The situation is inverted for $La_{1-x}Sr_xCoO_3$: the $\tilde{C}oO_6$ spher es are under-charged and the (La, Sr)$\tilde{O}_{12}$ spheres exhibit both under-charged and over-charged state.

For all cases, one can observe that when the spheres $\tilde{B}O_6$ develop closer to saturation level ( $\tilde{M}S \to 0$), th e $\tilde{A}O_{12}$ also come closer to this level, that is to say, when some charge flows away from $\tilde{B}O_6$ spheres, the $\tilde{A}O_{12}$ also receive some more charge and *vice-versa*. Evidently, this shift minimalizes the overall decline from sa turation of bonds forced by substitution. Note that the bonding saturation of $\tilde{B}O_6$ and $\tilde{A}O_{12}$ does not develop i n parallel with the average valences of these spheres. The average valence may decrease (see Table 6, $\langle v_A \rangle$ o

f $La_{1-x}Sr_xCoO_3$) while the sphere is going more saturated (see Table 9, $AO_{12}$ of $La_{1-x}Sr_xCoO_3$ or Fig.7, (La,Sr)$O_{12}$).

### 5.2. Saturated bond valence

The atomic valence associated with the saturated bond length $R_s$ is called the saturated bond valence, or fo r short the saturated valence $v_s$. These saturated valences can be calculated from the data listed in Table 9 acc ording to the formula $v_s = v/n = e^{(R_0-R_s)/B}$. The results are collected in Table 10.

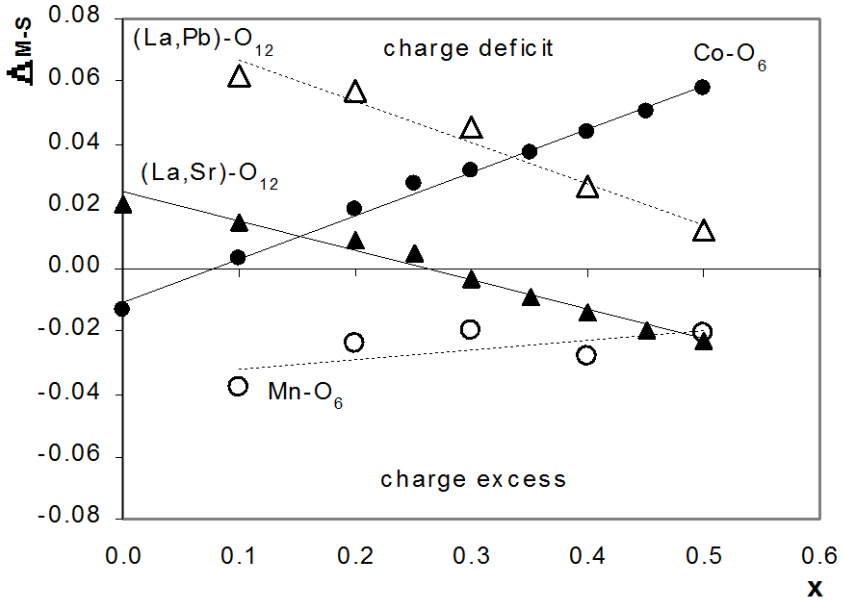


**Fig. 7. The linear dependences of $_{M-S}$ (difference between the me asured and the saturated bond lengths) on the content of substi tution x for $La_{1-x}Pb_xMnO_3$ and $La_{1-x}Sr_xCoO_3$. The draw for $La_{0.6}S r_{0.4-x}Ti_xMnO_3$ is omitted for clarity since it is similar to of $La_{1-x}Pb_x MnO_3$.**

The difference between measured and saturated valence is expressed as $v_{AS} = \langle v_A \rangle - v_s(AO_{12})$ and $v_{BS} = \langle v_B \rangle - v_s(BO_6)$ respectively. The total valence deviation $v$ of both spheres, calculated as $v = v_{AS} v_{BS}$ is drawn against the content of substitution $x$ in **Fig. 8**. This $v$ illustrates the balancing of the valence charg e between the spheres $BO_6$ and $AO_{12}$. As $v$ increases, the charge is shifted from $BO_6$ to $AO_{12}$ and *vice-vers a*.

For $La_{1-x}Sr_xCoO_3$ the graph crosses $x$ axis near $x \sim 0.15$. This means that at this substitution the coordinati on spheres of metals decline equally from the saturation, whereas for other cases the spheres are differently s aturated. The measure of this difference is expressed in the unit of electrons per unit cell and explores the asy mmetric distribution of the valence charge between the coordination spheres. The change of this measure des cribes the amount of charge flowed between them.

With content of $Sr^{2+}$ increased from 0 to 0.5 each sphere (La,Sr)$O_{12}$ in $La_{1-x}Sr_xCoO_3$ gained $|0.16 - 0.17| \sim$ 0.3e whereas the sphere $CoO_6$ lost $|0.50 - 0.11| \sim 0.6$e. At least 0.3e should be considered as shifted from $CoO_6$ to (La,Sr)$O_{12}$ although twice such amount has moved away from $CoO_6$. Here the substitution has mainly effe cted the $CoO_6$ spheres. For $La_{1-x}Pb_xMnO_3$ the (La,Pb)$O_{12}$ gained $|0.08 - 0.44| \sim 0.4$e and the $MnO_6$ lost $|0.20 - 0.33| \sim 0.1$e when content of $Pb^{2+}$ increased. The shifted amount of charge should be 0.1e. Here the substitution h ad more influence on (La,Pb)$O_{12}$ spheres than on the $MnO_6$. In $La_{0.6}Sr_{0.4-x}Ti_xMnO_3$ the spheres behaved simil arly as in $La_{1-x}Pb_xMnO_3$ if the substitution was taken in reverse order, i.e. from 0.25 downto 0.0. The charge d

eviation and charge shift were however nearly 3-4 times larger: |1.22 0.14| ~ 1.1e for (La,Sr,Ti)$O_{12}$ and |0.68 0.29| ~ 0.4e for $MnO_6$. Again, the $AO_{12}$ spheres have located more valence charge.

**Table 10. The deviation of the measured average bond valences from the saturated valences for the studied systems**

| | $x$ | $AO_{12}$ | | $BO_6$ | | $v$ |
|---|---|---|---|---|---|---|
| | | $v_s(AO_{12})$ | $v_{AS}$ | $v_s(BO_6)$ | $v_{BS}$ | |
| $La_{1-x}Pb_xMnO_3$ | 0.1 | 2.88 | -0.44 | 3.09 | 0.33 | -0.78 |
| | 0.2 | 2.77 | -0.40 | 3.18 | 0.21 | -0.61 |
| | 0.3 | 2.66 | -0.30 | 3.27 | 0.18 | -0.49 |
| | 0.4 | 2.56 | -0.17 | 3.37 | 0.26 | -0.44 |
| | 0.5 | 2.46 | -0.08 | 3.46 | 0.20 | -0.28 |
| $La_{0.6}Sr_{0.4-x}Ti_xMnO_3$ | 0.00 | 2.56 | -0.14 | 3.37 | 0.29 | -0.44 |
| | 0.05 | 2.69 | -0.37 | 3.27 | 0.34 | -0.72 |
| | 0.10 | 2.83 | -0.62 | 3.18 | 0.39 | -1.01 |
| | 0.15 | 2.97 | -0.84 | 3.09 | 0.46 | -1.30 |
| | 0.20 | 3.11 | -1.04 | 3.00 | 0.57 | -1.60 |
| | 0.25 | 3.26 | -1.22 | 2.91 | 0.68 | -1.91 |
| $La_{1-x}Sr_xCoO_3$ | 0.00 | 3.00 | -0.17 | 3.00 | 0.11 | -0.27 |
| | 0.10 | 2.88 | -0.11 | 3.09 | -0.02 | -0.09 |
| | 0.20 | 2.77 | -0.07 | 3.18 | -0.16 | 0.09 |
| | 0.25 | 2.72 | -0.04 | 3.23 | -0.23 | 0.19 |
| | 0.30 | 2.66 | 0.02 | 3.27 | -0.26 | 0.28 |
| | 0.35 | 2.61 | 0.06 | 3.32 | -0.32 | 0.38 |
| | 0.40 | 2.56 | 0.10 | 3.37 | -0.38 | 0.48 |
| | 0.45 | 2.51 | 0.14 | 3.42 | -0.43 | 0.57 |
| | 0.50 | 2.46 | 0.16 | 3.47 | -0.50 | 0.66 |

While both spheres in $La_{1-x}Pb_xMnO_3$ and $La_{0.6}Sr_{0.4-x}Ti_xMnO_3$ become closer to the saturation balance, the spheres in $La_{1-x}Sr_xCoO_3$ developed away from this level. The maximal total valence deviation $v$ was near 0.8e for $La_{1-x}Pb_xMnO_3$, 0.7e for $La_{1-x}Sr_xCoO_3$ and ~2e for $La_{0.6}Sr_{0.4-x}Ti_xMnO_3$.

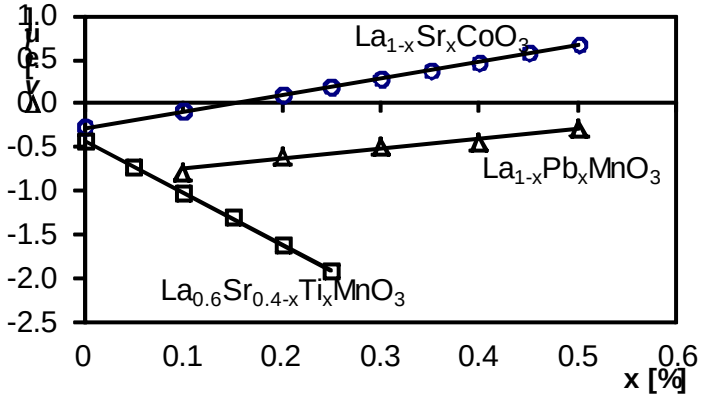


**Fig. 8. The strong linear dependences of v on substitution x show the balancing of valence charge in the spheres. The v is expressed in the unit of electrons per unit cell. The linearity also exists between the $v_{BS}$, $v_{AS}$ and x but we omit them here for clarity.**

The valence deviation from saturation of the spheres must be seen as the intrinsic bonding property of per ovskites. It forces the consideration that, by its nature the valence charge is polarized, although no such argu mentation is found in its definition. In all studied samples, the metals behave more-less like oppositely charg ed ions: the La, Pb, Sr, Ti are positive and the Co, Mn are negative. Since the valence charge are averaged ch arge, the real local charge asymmetries of the spheres can certainly deviate more than 2e/u from the saturatio n balance.

## 6. Problems and remarks

### 6.1. Resistibility to noise and accuracy of method

Since the determination of the coeficients $R_0$ was done statistically, the bond valence method is expected to have good resistibility to noise. The possible disturbance of results by the systematic or random errors (dur ing samples preparation, measurement and structure determination) is believed to be limited by the averaging of inputs when the $R_0$-s were determined. As tested and reported in [5], the bond valence method has accura cy around 5-7% for the ionic compounds. We have tested this method against the complex compounds (coval ence bonding character prevails) and found its accuracy was even a little better at 5-6%. Evidently, this accur acy does not depend on the physical meaning of bond valence but only on the statistical rules applying to the coeficients $R_0$ and B, i.e. on the process of averaging input data. Note that for perovskites the frequently men tioned Rietveld method provides $R_{Profile} \sim 10\%$. However, the bond valence method has one limitation just be cause of its statistical origin, that is it can not be applied everywhere *a priori*. The parameters obtained using one statistical file must not imply the correct results for the other files. This method is risky when using to an alyse one single case but is powerful for studying the collective effect of many samples.

### 6.2. The charge non-stoichiometry versus the real non-stoichiometry *x*

It is not clear how can the charge non-stoichiometry be associated with the real structure defects, although the occur ences of defects certainly affect. For the cases studied above, . does not imply any real defects. In principle, charge non -stoichiometry can happen in the perfect structures without any defects. The next analysis can illustrate.

By suggestion that the charge deficit was generated by the oxygen holes in the lattice, the holes density co uld be directly determined from. For example, = 0.16 e/u for $La_{0.7}Sr_{0.3}CoO_3$ (Table 6) means that every $n$= 12.5 unit cells produces 1 missing oxygen (since the oxidation state of the oxygens is $\tilde{2}$ and 2/0.16=12.5). So = $1/n$=0.08 (oxygen/unit cell). Now suggest that the holes are equally distributed inside lattice, so their cr oss links creat a mosaic network which divides the lattice into the domain areas with the boundaries laid on t hese links. The maximal diameter of the domains is thus $D = n \times \langle a \rangle = \langle a \rangle / . = 3.834 \times 12.5 = 47.9$Å (<*a*> is the average pseudo-cubic lattice constant). This system would limit the crystallite size and the final effect w ould be seen by the broadenning of the X-Ray diffraction. Fig.9 compares the crystallite size <D> determine d by the fourier analysis of the strongest diffraction and the domain diameter D for $La_{\tilde{1}x}Pb_xMnO_3$ and $La_{0.6}Sr_{0.\tilde{4}x}Ti_xMnO_3$. As seen, for both systems the crystallite size <D> follows linearly the content of substitution *x*, whereas the D develops differently. The sharp linear relationship between <D> and *x* for the studied cases is somehow surprising, although some weaker relationships have already been reported (e.g. see [11]). This lin earity can hardly be explained by the real defects. It is also not easier for the valence charge.

If we would agree to that a greater crystallite creates a larger flow place for the valence charge transfer, th e problem would look more acceptable. This would mean that the crystal growth always minimizes the decli ne from saturation of spheres and the final crystallite size corresponds to the strongest effect of this minimali zation (in given experimental conditions).

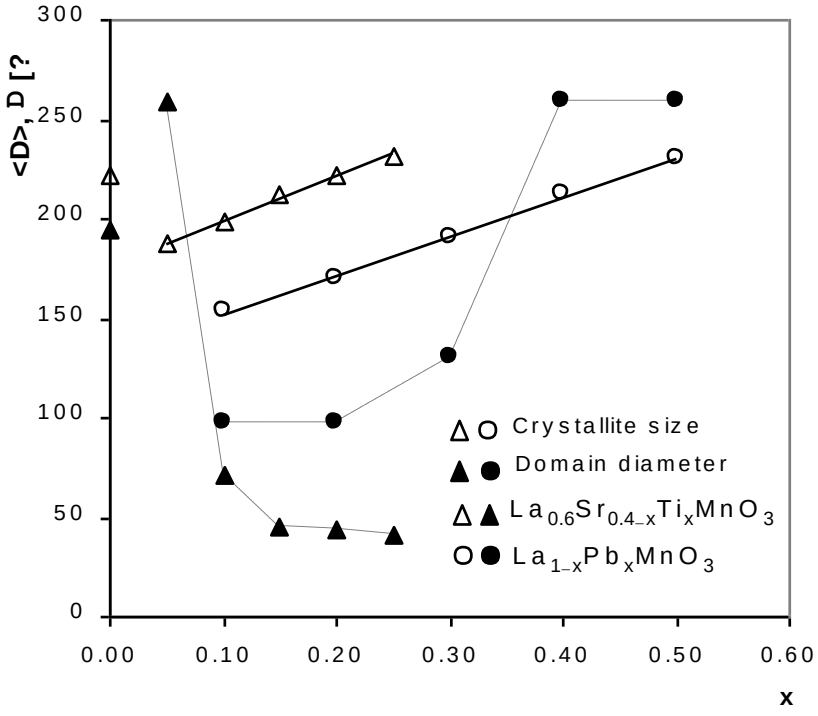


**Fig. 9. The crystallite sizes as determined from X-Ray study a nd the domain diameter D.**

### 6.3. Saturated bond valence and $B^{4+}$ concentration

The expected concentration of the cations $B^{4+}$ is equal to the content of substitution $x$ in the studied syste ms except for $La_{0.6}Sr_{0.4-x}Ti_xMnO_3$ where it is $0.4x$. The linear dependences $v_{BS}=f(x)$ and $v_{AS}=f(x)$ also mea n the linearity between $v_{BS}$, $v_{AS}$ and the expected concentration of $B^{4+}$.

If we now consider $|v_{BS}|$ as reflecting the real $B^{4+}$ content, then (*a*) for $La_{1-x}Sr_xCoO_3$ this content correlat es well with $x$ but does not exceed $x$ (Table 10, $v_{BS} < x$) so the exceeded amount of charge ( $v > x$ for $x$=0. 0, 0.35-0.50) comes from the $AO_{12}$ spheres (0.3e); (*b*) for the $La_{1-x}Pb_xMnO_3$ and the $La_{0.6}Sr_{0.4-x}Ti_xMnO_3$ this c ontent decreases merely when the stoichiometric concentration $Mn^{4+}$ increases, so the exceeded amount of ch arge (total $v > x$) again comes from the $AO_{12}$ spheres (0.1e, 1.1e); (c) the s.o.f.s of $Mn^{4+}$ reported in the Ta ble 2 & Table 4 agree better with the $v_B$ then with the stoichiometric concentration. Thus we can conclude here that for the studied cases the $v_B$ is closer to the real $B^{4+}$ concentration then the stoichiometric concentr ation.

### 6.4. Remark on anisotropy of valence charge

The concepts of charge are commonly divided into two types: the static charge and the dynamic charge. The valence charge corresponds to the static charge. Empirically and in symmetrical bonding spheres this ch arge cannot be polarized. But as has been showed here, it is asymmetrically located, so is polarized in the sca le that is not negligible. The valence charge polarization however does not come from any anisotropy in the *metal-oxygen* bonds, as for the dynamic charge, but from anisotropy in the triple bonding system *metal-oxyg ens-metal*. Note that the word "oxygens" is written in plural.

**Table 11. Comparison of the evolution of Born effective charges (1st r ow) and valence charge (2nd row) for $BaTiO_3$ under isotropic pressur e in cubic phase.Cell constant is listed in the first column.**

| *a[Å]* | $Z_{Ba}$ | $Z_{Ti}$ | $Z_{O\perp}$ | $Z_{O\parallel}$ | Z( /2) | $Z_{Ba}+Z_{Ti}$ | *v* |
|---|---|---|---|---|---|---|---|

| | | | | | | | |
|---|---|---|---|---|---|---|---|
| 3.64 | 2.95 | 7.23 | -2.28 | -5.61 | -3.95 | 10.18 | |
| | 5.49 | 5.92 | | | -3.80 | 11.41 | 1.58 |
| 3.94 | 2.77 | 7.25 | -2.15 | -5.71 | -3.93 | 10.02 | |
| | 3.10 | 3.95 | | | -2.35 | 7.04 | 1.15 |
| 4.00 | 2.74 | 7.29 | -2.13 | -5.75 | -3.94 | 10.03 | |
| | 2.76 | 3.64 | | | -2.13 | 6.40 | 1.13 |
| 4.40 | 2.60 | 7.78 | -2.03 | -6.31 | -4.17 | 10.38 | |
| | 1.29 | 2.12 | | | -1.14 | 3.41 | 1.17 |

The Double-Exchange mechanism, frequently used to discuss the magnetic behaviour of perovskites, follows from the simple triple bonding system metal-oxygen-metal (e.g. MnOMn). The valence charge polarization depends on anisotropy of the whole *chain of bonding spheres*, not of single bonds and is measured by *v*. Table 11 compares the sensitivity of the valence charge and the dynamic charge to the structural changes for $BaTiO_3$. The calculation of the dynamic charges come from [27]. The studies on valence charge polarization may lead to explanation of many interesting properties of perovskites.

## 7. Conclusion

We have demonstrated the usefulness of the pseudo-cubic lattices to perovskites and have determined such structures for two perovskite systems $La_{1-x}Pb_xMnO_3$ ($x$=0.00.5) and $La_{0.6}Sr_xTi_{0.4x}MnO_3$ ($x$=0.00.25). The revision of the structures $La_{1-x}Sr_xCoO_3$ ($x$=0.00.5) have also been made. The pseudo-cubic lattice is usually sensitive to the angular deformation, so is suitable for the study of small angular deformation in the perovskite lattices. Based on the crystal structure data, a systematic study of valence charge was made together with the theoretical model for retrieving the valence charge information directly from the pseudo-cubic lattices. Several conclusions can be made as followed:

(*a*) The charge non-stoichiometry parameter was always positive and did not reach above 0.02 in the studied systems. No association of this . and the real formula stoichiometry *x* has been observed. This charge non-stoichiometry . should occur also in the perfect crystals where the formula would be exactly $ABO_3$.

*b*) All studied perovskites showed the *valence charge deficit* in the unit cell. The clear evidence of this was that there was no visible contraction of the lattice constants in the given systems when the total valence charge in the unit cell increased (i.e. when the non-stoichiometry parameter →0). This demonstrates the failure of distortion theorem in all these systems.

(*c*) In all studied samples the valence charge was *asymmetrically localized* - with respect to the saturation balance of the bond distances, between the coordination spheres $AO_{12}$ and $BO_6$. The dependence of $_{M-S}$ (the difference between the measured and the saturated bond lengths) on the content of substitution *x* was clearly linear.

(*d*) As the content of substitution *x* varied, a certain *charge transfer process* between the coordination spheres $AO_{12}$ and $BO_6$ was seen - with respect to the saturation balance of the bond valences. This process is strongly linear to the substitution, as was demonstrated by the linear relationship between the total valence deviation *v* and the content of substitution *x* ($R^2$~1). The shifted charge was from 0.1e to 1.1e per unit cell.

This work involved the theoretical concepts of the saturated bond length and the saturated bond valence. In general they coincide with the statistical averages of the bond lengths and the bond valences of the same bonds. The declines from these average levels signify the state of being under-charged or over-charged of the bonds. In certain aspect these levels mark the bond ability to absorb more electron. With respect to them, a certain internal charge transfer process between the coordination spheres of the metals has been observed. How this process changes under the specific conditions is still the question.

## Acknowledgement

The author would like to thank the Center for Materials Science, Faculty of Physics, HUS-VNU for providing materials and kind helps during measurement and other experimental works. Especial thank is expressed to Prof. Nguyen Chau for fruitful discussions and supports.

## References


[1] I.D. Brown, *Structure and Bonding* 2, Springer-Verlag 1981.
[2] L. Pauling, *J. Amer. Chem. Soc.* 51, 1010 (1929)
[3] L. Pauling, *Nature of Chemical Bonds*, 3rd ed., Cornell University Press, Ithaca, NY, 1960.
[4] D. Altermatt, I.D. Brown, *Acta Cryst*. B41, 244 (1985)
[5] I.D. Brown, R.D. Shannon, *Acta Cryst.* A29, 266 (1973)
[6] T. Ito, *Maruzen*, Tokyo 187 (1950)
[7] J.V. Visser, *J. Appl. Cryst*. 2, 89 (1969)
[8] D. Taupin, *J. Appl. Cryst.* 21, No.Pt5, 485 (1988)
[9] W.H. Zachariasen, *Acta Cryst.* 16, 385 (1963)
[10] Jouanneaux, "WinMProf : a visual Rietveld software", *CPD newsletter* 21, 13 (1999)
[11] T. Tao, Q.Q.Cao, K.M.Gu, H.Y.Xu, S.Y.Zhang and Y.W.Du, *Appl.Phys.Letters* 77, No.5, 723 (2000)
[12] S.L.Ye, H.Song, J.M.Dai, K.Y.Wang, J.J.Du, Y.P.Sun, J.Fang, J.L.Chen and B.J.Gao, *J.Appl.Phys.* 90, No.6, 2943 (2001)
[13] D.P. Fagg, J.C. Waerenborgh, V.V. Kharton, J.R. Frade, *Solid State Ionics* 146, 87 (2002)
[14] T.K.Solovykh, I.O.Troyanchuk, D.D.Khalyanvin, H.Szymczak and K.Piotrowski, *Phys.Stat. Sol. (a)* 17 2, 485 (1999)
[15] Y. Ohno, S. Nagata, H. Sato, *Solid State Ionics* 9, 1001 (1983)
[16] Ohbayashi, *Jpn. J. Appl. Phys*. 13, 1 (1974)
[17] L.T.C.Tuong, P.V.Phuc, N.N.Toan, *Proceedings of the Third IWOMS'99,* Hanoi, Vietnam, 399 (1999)
[18] Hoang Nam Nhat, *Proceedings of the VGS5*, Hanoi, Vietnam, 2001 (To be published)
[19] N. Chau, N.H.Luong, D.L.Minh, N.D.Tho and N.N.Chau, *Research Reports in Physics*, Hanoi Universit y of Sciences Preprint Series, Vol. 1, No. 8, 1 (2002)
[20] C.W.Searle and S.T.Wang, *Can.J.Phys.* 47, 2703 (1969)
[21] C.W.Searle and S.T.Wang, *Can.J.Phys.* 48, 2203 (1970)
[22] Ting-Sheng Huang, Chiung-Hsiung Chen and Ming-Fong Tai, *Mat.Res.Soc.Symp.Proc.*, Vol. 674, U3.4. 1-U.3.4.6 (2001)
[23] J.M.D.Coey, M.Viret and S.von Molna, *Advances in Physics* 48, 167 (1999).
[24] M.E.Melo Jorge, A.Correia dos Santos, M.R.Nunes, *Int. J. of Inorganic. Materials* 3, 915 (2001)
[25] C.N.R.Rao and A.K.Raychaudhuri, *Colossal Magnetoresistance. Charge Ordering and Other Novel Pr operties of Manganates and Related Materials*, World Scientific, Singapore, 1998.
[26] R.D. Shannon and C.T. Prewitt, *Acta Cryst. Sect. A: Cryst.Phys., Diffr., Theor.Gen. Cryst.* 32, 785 (197 6)
[27] Ph. Ghosez, J-P. Michenaud and X. Gonze, *Phys. Rev. B* 58, No.10, 6224 (1998)
[28] Donnay, G., Allman, R. *Amer. Min.* 55, 1003 (1970)
[29] Donnay, G., Donnay, J.D.H., *Acta Cryst.* B29, 1417 (1973)
[30] Bystrom, A., Wilhelmi, K.A., *Acta Chem. Scand.* 5, 1003 (1951)
[31] Clark, J.R., Appleman, D., Papike, J., *Min. Soc. Amer. Spec. Paper* 2, 31 (1969)
[32] Y.L. Chang, Q. Hoang, C.K. Ong, *J. Appl. Phys.* 91, 789 (2002)